



OPEN

## Changes in the transcriptomic profile of cumulus cells under the influence of cumulus-oocytes complex pre-incubation

Azam Govahi<sup>1,6</sup>, Sahar Eghbali<sup>2,6</sup>, Naser Elmi Ghiasi<sup>3</sup>, Zahra Zandieh<sup>4</sup>, Marziyeh Ajdary<sup>1</sup>, Rana Mehdizadeh<sup>5</sup> & Mehdi Mehdizadeh<sup>4</sup>✉

Pre-incubation of the cumulus-oocyte complex (COCs) may lead to better function of cumulus cells (CCs) and higher oocyte quality by changing the transcriptomic profile of CCs. 140 cumulus cell samples were isolated from 12 participants and divided into two groups based on pre-incubation time. In the T0 group, the COCs were immediately dissected to separate the CCs from around the oocytes. In the T2 group, CCs were prepared after 2 h of incubation. Then, the transcriptomic profile of the CCs of the non pre-incubation group was compared to the 2-h pre-incubation group. Confirmation of RNA sequencing results was done via qRT-PCR. The CCs transcriptome analysis showed 17 genes were downregulated and 22 genes upregulated in the T2 group compared to the T0 group. Also, the pathways related to ATP production (oxidative phosphorylation, electron transport chain, and Mitochondrial complex I assembly model OXPHOS system), TNF-alpha signaling pathway, and glucocorticoid receptor pathway increased in the T2 group compared to the T0 group. Also, the TGF- $\beta$  pathway was decreased in the T2 group compared to the T0 group. This study showed that 2 h pre-incubation leads to changes in important pathways in CCs, which positively affects oocyte quality.

**Keywords** Pre-incubation, Cumulus cells, RNA-sequencing, Oocyte quality

According to reports, 10–15% of couples worldwide are infertile<sup>1</sup>. Among the standard techniques for treating infertility is intracytoplasmic sperm injection (ICSI)<sup>2</sup>. In the ICSI technique, the oocytes collected from the individual are incubated until the ICSI is performed (Pre-incubation), and this incubation time varies depending on the specific conditions of the laboratory<sup>3</sup>. The evidence is that the complete and final maturation of the nucleus and cytoplasm of the oocyte is necessary for its activation by sperm and also plays a significant role in embryo quality<sup>3</sup>. Since cytoplasmic maturation of oocytes takes more time than nuclear maturation, oocyte pre-incubation may lead to coordination between them<sup>4</sup>.

Although there are many differences of opinion regarding the necessity of pre-incubation, and some studies have shown that pre-incubation of oocytes does not affect fertility or pregnancy outcome<sup>5</sup>, in some studies, it has been stated that the pre-incubation of oocytes before ICSI plays a role in completing the nuclear and cytoplasmic maturation of the oocyte<sup>5,6</sup>. On the other hand, in pre-incubation, attention should be paid to the passage of time and oocyte aging and its effect on reducing oocyte quality and fertilization rate<sup>4</sup>. In investigating the impact of different periods of oocyte pre-incubation on nucleus maturation, fertility rate, and embryo quality in IVF and ICSI, 176 IVF and 64 ICSI cycles were studied, and the results showed that at least 2.5 h of pre-incubation is beneficial for IVF and ICSI due to increasing the maturation of oocytes<sup>5</sup>. In the study comparing zero and 2–4 h of oocyte pre-incubation before ICSI, 2–4 h pre-incubation improved oocyte and embryo quality<sup>6</sup>. But,

<sup>1</sup>Endometriosis Research Center, Iran University of Medical Sciences, Tehran, Iran. <sup>2</sup>Department of Anatomy, School of Medicine, Iran University of Medical Sciences, Tehran, Iran. <sup>3</sup>Laboratory of Complex Biological Systems and Bioinformatics (CBB), Institute of Biochemistry and Biophysics (IBB), University of Tehran, Tehran, Iran. <sup>4</sup>Reproductive Sciences and Technology Research Center, Department of Anatomy, Iran University of Medical Sciences, Tehran, Iran. <sup>5</sup>School of Dentistry, Central Tehran Branch, Islamic Azad University, Tehran, Iran. <sup>6</sup>These authors contributed equally: Azam Govahi and Sahar Eghbali. ✉email: mehdizadeh.m@iums.ac.ir

pre-incubation for more than 4 h led to a decrease in oocyte quality<sup>4</sup>. The study results of the effect of different pre-incubation times (from half to 6 h) on the fertilization rate following ICSI showed that the fertilization rate in different time groups before ICSI do not differ significantly from each other<sup>7</sup>. Therefore, it seems necessary to investigate the appropriate pre-incubation time and its effect on oocyte quality. The issue to be considered is the minimum pre-incubation time required for oocyte maturation and the maximum pre-incubation time that does not lead to oocyte senescence.

In folliculogenesis, the communication between the oocyte and its surrounding granulosa cells, cumulus cells (CC), is critical for oocyte maturation<sup>8</sup>. The inner row of CC is connected to the zona pellucida of the oocyte, and by establishing a connection with the cytoplasmic membrane, they form the cumulus-oocyte complex (COC), which has three types of connections. One of these communications is the gap junctions that transfer small molecules between the oocyte and the CC. In addition, paracrine signals between these two types of cells are also necessary for the growth and regulation of oocyte meiotic maturation<sup>9</sup>. Another connection is the production of part of the follicular fluid by the CC, which can also its effects on the oocyte<sup>10</sup>. Also, the factors secreted from oocytes affect the gene expression and protein pattern of CC. Therefore, CC can reflect the quality of oocytes and a suitable method for selecting or examining oocytes<sup>8</sup>.

Since there is a difference of opinion about the time of pre-incubation and most of the studies conducted are clinical and little molecular research has been done in this direction, also, because the direct examination of the oocyte is not ethical, in this study, the changes in the transcriptomic profile of cumulus cells under the influence of two time zero and T2 pre-incubation of human COC in patients treated in ART cycles and pathways involved in this process were investigated.

## Materials & methods

### Patient selection and ovulation stimulation

The study approval was obtained from the Ethics Committee of Iran University of Medical Science (Reference number: IR.IUMS.REC.1396.31837), and all research was performed by relevant guidelines. Written consent was obtained from all participants. 12 healthy oocyte donor women (with at least one natural pregnancy resulting in a live birth) were included in the study. The BMI of all participants was in the normal range (between 18 and 28) with a mean ( $\pm$  SD) age of less than 35 ( $31.80 \pm 3.07$ ). Also, the antagonist protocol was used to stimulate ovulation in all of them.

### COC Pre-incubation and cumulus cell isolation

The collection of COCs was done 36–38 h after hCG administration with ultrasound-guided transvaginal puncture. Then, the COCs were washed with GMOPS medium (Vitrolife, Gothenburg, Sweden) to remove the blood contamination. At this stage, the COCs were divided into T0 and T2 groups. In the T0 group, COCs were immediately dissected to separate the cumulus cells from around the oocytes and prepare the oocytes for ICSI. Then, cumulus cells related to mature metaphase II (MII) oocyte were centrifuged at 200 g for 10 min after washing with phosphate-buffered saline (PBS) stored in liquid nitrogen. In the T2 group, dissection and preparation of cumulus cells were done after 2 h of COC incubation. Pre-incubation was performed at 37 °C, 95% humidity, 6% CO<sub>2</sub>, and 5% O<sub>2</sub> condition. All the media were from Vitrolife (Vitrolife, Gothenburg, Sweden). Cumulus cells related to MII oocytes were used in this study.

### RNA-seq and bioinformatics analysis

140 CC samples were isolated from 12 patients and divided into two groups based on pre-incubation time. 70 samples were placed in each group. 40 samples from each group were used for RNA-Seq, and the remaining 30 samples were used to confirm the RNA-Seq results via qRT-PCR.

Extracted RNA has been sequenced by BGI Hong Kong using an rRNA depletion stranded library preparation kit. More than 13 GB of sequences were generated with Q20 percent more than 97% with 100bp length in PE mode using the DNBseq sequencing platform. We used FastQC<sup>11</sup> to double-check the quality of raw data. Since the Phred score of the reads was more than almost 30 for all positions and there were no contaminations, there was no need for trimming and adaptor removal. Next, the Hisat2 algorithm on the GRCh38/hg38 human reference genome was used for alignment<sup>12</sup>. We also downloaded the RefSeq gtf file for the hg38 reference build from the UCSC database. Next, the aligned outputs from Hisat2 were sorted using Samtools. Then, the set of expressed transcripts and differentially expressed genes were identified using Stringtie and cuffdiff tools<sup>13,14</sup>. Note that in cuffdiff fragments per kilobase of transcript per million mapped reads (FPKM), library normalization and blind dispersion method were used. It is worth mentioning that this algorithm has been specially developed for cases with no replicates. Next, significantly differentially expressed genes (DEGs) for this study were extracted based on the FDR corrected  $P$  value  $< 0.05$  and  $|\log_2(\text{FC})| > 1$  condition. Then, the statistical power of our test was estimated using the average depth of covering the expressed genes and *rnapower* function from the *RNASeqPower* package<sup>15</sup>. Finally, the gene ontology terms and pathway enrichment analysis of significantly upregulated and down-regulated genes were done using the EnrichR online database<sup>16</sup>. Integrated Genome Viewer (IGV) tools were used to visualize genes selected for validation using RT-qPCR<sup>17</sup>.

In the following, the pathways associated with the human cumulus cells in the patients treated in ART cycles influenced by two time zero and T2 pre-incubation were studied. Considering the related enriched pathways to this research, especially in WikiPathway terms and other enrichment analyses such as biological process gene ontology terms and KEGG pathway analysis, four candidates from upregulated and downregulated DEGs genes were selected for qRT-PCR validation.

### qRT-PCR validation

The qRT-PCR method was used to confirm the RNA sequencing data. 4 genes were selected for confirmation: genes *CXCL8* (C-X-C motif chemokine ligand 8), *TNFAIP3* (TNF alpha-induced protein 3), and *ND5* (mitochondrially encoded NADH dehydrogenase 5) had the highest expression, and gene *EGR2* (early growth response 2) had the lowest expression in the T2 group compared to the T0 group. 30 samples of each group were used for confirmation of RNA-Seq results via qRT-PCR.

Total RNA was extracted using the RNeasy Mini kit (Qiagen, Germany). Triplicate technical replicates were considered for all samples. The A260/A280 ratio of samples was assessed by a Nanodrop spectrophotometer, and concentration and purity was examined. According to the manufacturer's instructions and via the High Capacity cDNA Reverse Transcription Kit (Bio-Rad, 1,725,037) Random Hexamer primers, reverse transcription was done. ABI Prism 7300 Sequence Detector (Applied Biosystems, Foster City, California, USA) was used for qPCR reactions. Standard curves were checked out, and 'Primers' Efficiency was confirmed. The sequence of primers is shown in Table 1. Then, the relative transcript levels (Life Science, 7900HT) were determined using the SYBR Green master mix and Sequence Detection System. Data normalization was done via human *GAPDH* housekeeping gene. Relative gene expression was quantified using  $\Delta\Delta$  the Ct method and calculated with  $FC = 2^{-\Delta\Delta CT}$  formula<sup>18</sup>.

### Statistical analysis

One-way ANOVA and 'Tukey's multiple comparisons test as post hoc were used for statistical analyses. Also, version 24.0 (IBM) of the SPSS and Prism 8 software were used.  $P < 0.05$  was statistically significant.

### Ethical approval

The study was approved by the Ethics Committee of Iran University of Medical Science (Reference number: IR.IUMS.REC.1396.31837).

## Results

### Bioinformatics analysis

DEGs analysis ( $q$  value  $< 0.05$  and  $|\log_2(FC)| > 1$ ) resulted in the identification of 39 genes, including 22 upregulated genes and 17 downregulated genes. Tables 2 and 3 shows the upregulated and downregulated genes, respectively. Moreover, in Fig. 1, the volcano plot of expressed genes is depicted. Based on Fig. 1, the dispersion of upregulated and downregulated genes and differentially expressed genes are almost the same. Finally, the statistical power of our test was estimated at  $0.8145 > 0.8$ . So, the sample size for the pooled samples was sufficient to expect statistically meaningful results.

It is worth mentioning that since our samples were pooled and we did not have replicates, the blind dispersion method from the Cuffdiff tool was used to estimate the p-values; as a result, p-value magnitudes were not widely dispersed. Next, a bubble plot was used to demonstrate the expression pattern of differentially expressed gene, as shown in Fig. 2.

In the next step, enrichment analysis was used to decipher the genes associated with the difference between the two sample groups and shed light on the molecular mechanism of the alteration between the two groups. The WikiPathway enrichment analysis results for upregulated and down-regulated genes are presented in the Tables 4 and 5, respectively.  $s$  of less than 0.05 were kept. Only the statistically significant terms with FDR corrected  $P$  values of less than 0.05 were kept in this analysis. In Fig. 3, the expression level of the candidate genes in this study is shown. Note that the expression levels have been normalized using FPKM, and the  $P$  value corrected using the false discovery method.

### qRT-PCR

RNA-Seq results were confirmed by using CCs from both groups. The results of qRT-PCR were shown the expression of *CXCL8*, *TNFAIP3*, and *ND5* genes in the T2 group were significantly higher than in the T0 group

Gene	Primer (5-3)	Tm	Product length	Gene ID
<i>CXCL8</i>	Forward: ATGGCTGCTGAACCACTAGA	58.72	570	3576
	Reverse: CTAGTCTTCGTTTGAACAG	51.93		
<i>TNFAIP3</i>	Forward: AGAGCAACTGAGATCGAGCCA	61.23	145	7128
	Reverse: CTGGTTGGGATGCTGACACTC	60.95		
<i>ND5</i>	Forward: CAGCAGCCATTCAAGCAATGC	61.33	167	4540
	Reverse: GGTGGAGACCTAATGGGCTGATTAG	62.87		
<i>EGR2</i>	Forward: CTTGACCAGATGAA CGG AGT	57.95	100	1959
	Reverse: AGCAAAGCTGCTGGGATATG	58.31		
<i>GAPDH</i>	Forward: GCAGGGATGATGTTCTGG	55.07	126	2597
	Reverse: CTTTGGTATCGTGAAGGAC	55.86		

**Table 1.** Sequences of the primers used in this study.

Gene symbol	Locus	Expr(0 h)	Expr(2 h)	Log2(FC)	P_value	FDR
CSF3	chr17:40,015,439–40,017,813	0	0.782705	inf	5.00E–05	0.023765
FAM163A	chr1:179,591,612–179,819,418	0	0.563185	inf	5.00E–05	0.023765
SERPINB2	chr18:63,885,285–63,903,888	0	1.78659	inf	5.00E–05	0.023765
MTATP6P1	chr1:633,534–634,922	18.3315	69.3245	1.91904	5.00E–05	0.023765
HSD3BP3	chr1:119,538,420–119,546,244	0	0.909862	inf	5.00E–05	0.023765
TET3	chr2:73,983,630–74,147,912	17.3608	76.2401	2.13472	5.00E–05	0.023765
PTX3	chr3:157,173,699–157,503,605	27.6991	94.4144	1.76917	5.00E–05	0.023765
CXCL8	chr4:73,740,568–73,743,716	13.963	82.2564	2.55852	5.00E–05	0.023765
AREG	chr4:74,445,135–74,455,005	72.8527	215.467	1.56441	0.0001	0.039793
RGS4	chr1:163,068,870–163,076,802	10.896	39.5985	1.86165	5.00E–05	0.023765
IL7R	chr5:35,856,890–35,879,603	8.19245	31.4328	1.93991	5.00E–05	0.023765
TNFAIP3	chr6:137,823,668–137,883,312	38.3909	142.782	1.89498	5.00E–05	0.023765
INHBA	chr7:41,685,113–41,779,378	5.927	27.246	2.20067	5.00E–05	0.023765
ND1	chrM:3306–4262	107.37	472.212	2.13684	5.00E–05	0.023765
ND2	chrM:4469–5511	64.4693	322.528	2.32274	5.00E–05	0.023765
ND3	chrM:10,058–10,404	125.611	568.492	2.17818	5.00E–05	0.023765
ND4	chrM:10,469–12,137	208.316	842.433	2.01579	5.00E–05	0.023765
ND5	chrM:12,336–14,148	105.397	375.965	1.83477	5.00E–05	0.023765
ND6	chrM:14,148–14,673	25.7703	99.2931	1.94598	0.0001	0.039793
BIRC3	chr11:102,317,483–102,339,403	2.65885	12.9447	2.28349	5.00E–05	0.023765
NFATC2	chr20:51,366,434–51,562,839	0.373128	2.72307	2.86749	0.0001	0.039793
TNFRSF18	chr1:1,203,507–1,206,592	0	0.703968	inf	5.00E–05	0.023765

**Table 2.** Upregulated DEG in T2 group compared to T0 group.

Gene symbol	Locus	Expr(0 h)	Expr(2 h)	Log2(FC)	P_value	FDR
IER2	chr19:13,150,410–13,154,911	180.057	60.8156	–1.56594	0.0001	0.039793
MIR23A	chr19:13,834,515–13,842,918	26.8313	7.52007	–1.8351	5.00E–05	0.0237653
EGR4	chr2:73,290,928–73,293,548	37.651	8.33332	–2.17572	5.00E–05	0.0237653
SLC40A1	chr2:189,560,589–189,580,786	30.8014	6.76107	–2.18767	5.00E–05	0.0237653
GJA5	chr1:147,700,065–147,789,690	86.6778	24.6572	–1.81366	5.00E–05	0.0237653
OXTR	chr3:8,733,801–8,769,613	37.7563	12.6232	–1.58064	5.00E–05	0.0237653
BMP3	chr4:81,030,707–81,057,627	45.746	14.8048	–1.62758	5.00E–05	0.0237653
NPY2R	chr4:155,173,722–155,217,076	12.8719	2.80762	–2.1968	5.00E–05	0.0237653
SOX4	chr6:21,593,750–21,598,619	70.8297	11.2543	–2.65388	5.00E–05	0.0237653
H3C2	chr6:26,031,588–26,032,099	83.8249	21.6336	–1.95411	0.0001	0.039793
FAM78A	chr9:131,258,077–131,281,045	26.7168	8.1076	–1.7204	5.00E–05	0.0237653
EGR2	chr10:62,811,995–62,819,167	47.4673	12.0846	–1.97376	5.00E–05	0.0237653
ID3	chr1:23,539,882–23,573,700	69.8879	11.9376	–2.54953	5.00E–05	0.0237653
FOS	chr14:75,278,827–75,282,230	939.748	263.795	–1.83286	0.0001	0.039793
SMAD6	chr15:66,702,235–66,782,849	21.9378	3.62308	–2.59813	5.00E–05	0.0237653
MEX3B	chr15:82,041,777–82,046,018	24.3927	5.49967	–2.14903	5.00E–05	0.0237653
CDH3	chr16:68,645,309–68,733,771	7.28527	1.34714	–2.43508	5.00E–05	0.0237653

**Table 3.** Down-regulated DEG in T2 group compared to T0 group.

(\* $P < 0.05$  / \*\* $P < 0.01$  / \*\*\* $P < 0.001$  / \*\*\*\* $P < 0.0001$ ). *EGR2* gene expression in the T2 group was significantly lower than the T0 group (\*\*\*\* $P < 0.0001$ ) (Fig. 4).

## Discussion

In this study, the transcriptomic profile of CCs corresponding to T2 pre-incubated COCs with non-incubated COCs were compared. The results showed that a series of genes and pathways have changed in the CCs of the T2 group compared to the T0 group. Among the most important of them were the paths related to ATP production (oxidative phosphorylation, electron transport chain, and Mitochondrial complex I assembly model OXPHOS system), TNF-alpha signaling pathway, and glucocorticoid receptor pathway, which increased in the T2 group compared to the T0 group. Also, the TGF- $\beta$  pathway was decreased in the T2 group compared to the T0 group.

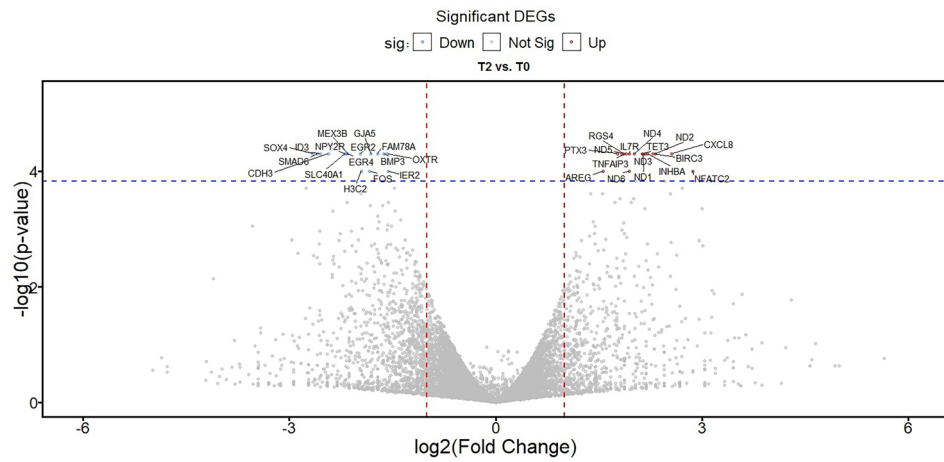


**Figure 1.** Volcano plot for DEGs between the T2 group and T0 group.

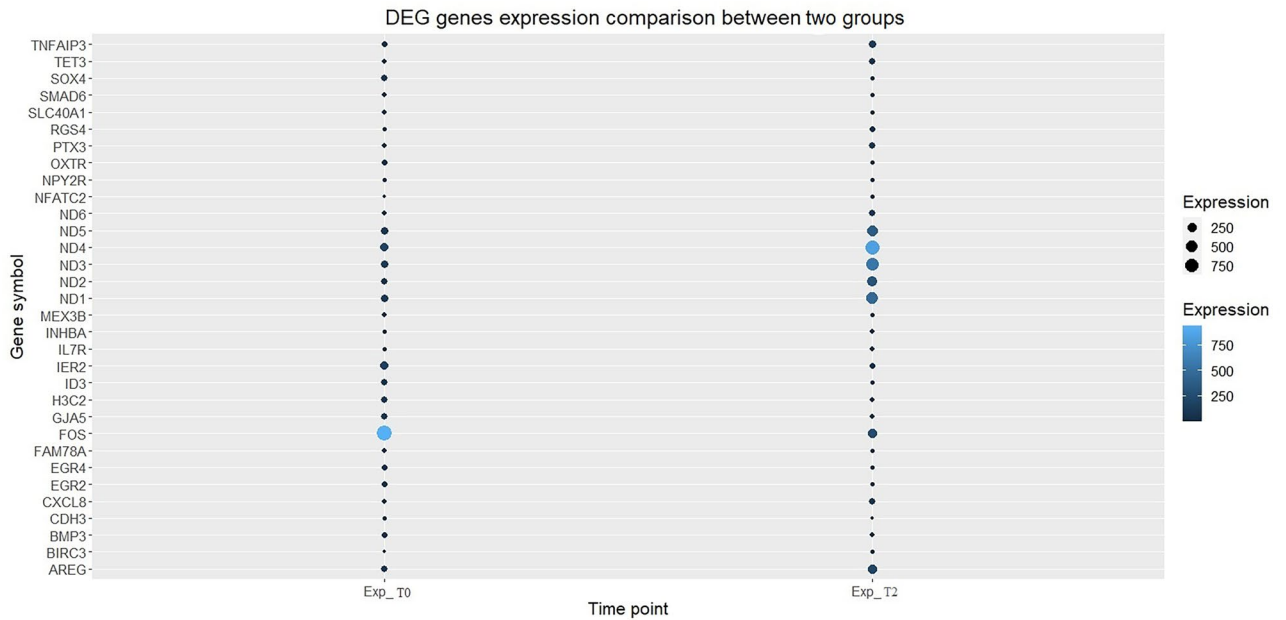


**Figure 2.** Gene expression pattern between two groups for DEG.

Enriched pathway Term (WikiPathway)	q-value	Combined score	Genes
Oxidative phosphorylation WP623	3.28E-09	3310.898281	ND6;ND1;ND3;ND2;ND5;ND4
Electron Transport Chain (OXPHOS system in mitochondria) WP111	4.55E-08	1583.835259	ND6;ND1;ND3;ND2;ND5;ND4
Mitochondrial complex I assembly model OXPHOS system WP4324	9.83E-08	2233.049633	ND6;ND1;ND2;ND5;ND4
Senescence and Autophagy in Cancer WP615	0.002335	261.8466943	SERPINB2;CXCL8;INHBA
Gastrin signaling pathway WP4659	0.002599	233.6510707	SERPINB2;CXCL8;BIRC3
Thymic Stromal LymphoPoietin (TSLP) Signaling Pathway WP2203	0.009694	297.4766814	CXCL8;IL7R
Hematopoietic Stem Cell Differentiation WP2849	0.011176	240.7359739	CSF3;NFATC2
Glucocorticoid Receptor Pathway WP2880	0.016611	173.5450943	TNFAIP3;BIRC3
TNF-alpha signaling pathway WP231	0.026347	119.1462592	TNFAIP3;BIRC3
Nuclear Receptors Meta-Pathway WP2882	0.026697	52.16380457	SERPINB2;TNFAIP3;BIRC3
Cytosine methylation WP3585	0.048188	549.1072571	TET3
Regulation of toll-like receptor signaling pathway WP1449	0.048188	66.53066798	TNFAIP3

**Table 4.** Enriched Wiki-Pathway terms for upregulated DEGs in T2 group compared to T0 group.

Enriched pathway term (WikiPathway)	q-value	Combined score	Genes
Adipogenesis WP236	0.006401258	290.6570558	BMP3;EGR2;ID3
TGF-beta Receptor Signaling WP560	0.020494571	355.7433228	FOS;SMAD6
TGF-beta receptor signaling in skeletal dysplasias WP4816	0.020494571	323.519069	FOS;SMAD6
Peptide GPCRs WP24	0.026577362	233.6130223	OXTR;NPY2R
ESC Pluripotency Pathways WP3931	0.048946823	126.7131058	FOS;SMAD6
Regulation of toll-like receptor signaling pathway WP1449	0.048946823	98.52423894	FOS;SMAD6
Brain-derived neurotrophic factor (BDNF) signaling pathway WP2380	0.048946823	93.75610919	EGR2;FOS
Myometrial relaxation and contraction pathways WP289	0.048946823	83.74321389	OXTR;FOS
Iron metabolism in placenta WP2007	0.048946823	520.8353408	SLC40A1
Bone morphogenic protein (BMP) signaling and regulation WP1425	0.048946823	520.8353408	SMAD6
Neuroinflammation WP4919	0.048946823	469.1243344	FOS
Transcriptional cascade regulating adipogenesis WP4211	0.048946823	469.1243344	EGR2
ncRNAs involved in STAT3 signaling in hepatocellular carcinoma WP4337	0.048946823	469.1243344	SOX4
H19 action Rb-E2F1 signaling and CDK-Beta-catenin activity WP3969	0.048946823	425.939424	SOX4
ID signaling pathway WP53	0.048946823	358.0671609	ID3
MAPK pathway in congenital thyroid cancer WP4928	0.048946823	358.0671609	FOS

**Table 5.** Enriched Wiki-Pathway terms for down-regulated DEGs in T2 group compared to T0 group.

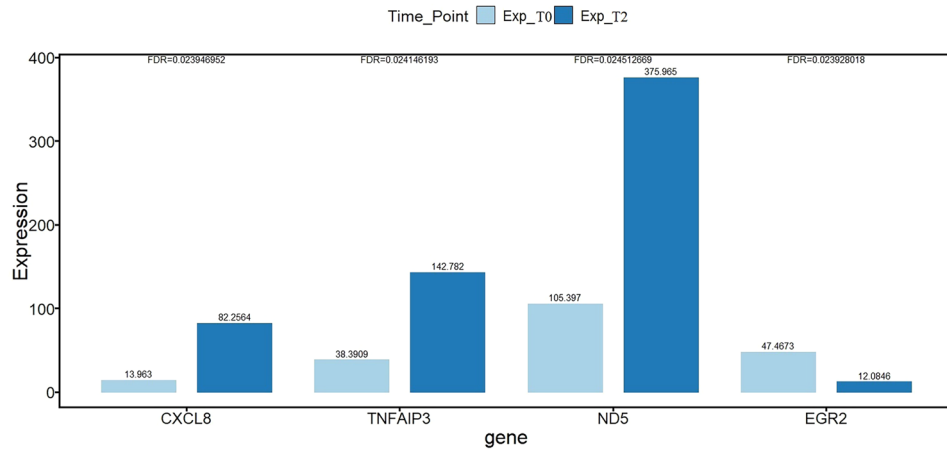


**Figure 3.** Comparison of normalized gene expression level for the candidate genes for qRT-PCR.

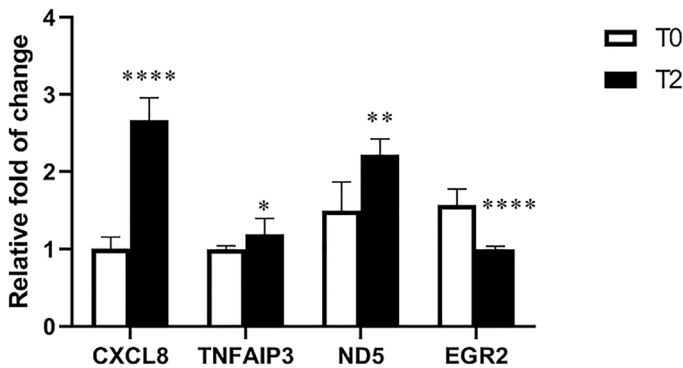


**Figure 4.** Relative expression of *CXCL8*, *TNFAIP3*, *ND5*, and *EGR2* genes in CCs of the T2 group compared with the T0 group. *CXCL8*: C-X-C motif chemokine ligand 8. *TNFAIP3*: TNF alpha-induced protein 3. *ND5*: mitochondrially encoded NADH dehydrogenase 5. *EGR2*: early growth response 2. (\* $P < 0.05$ / \*\* $P < 0.01$ / \*\*\* $P < 0.001$ / \*\*\*\* $P < 0.0001$ ).

In this study, the oxidative phosphorylation, electron transport chain or oxidative phosphorylation system (OXPHOS) in mitochondria, and the complex I system (Mitochondrial complex I assembly model OXPHOS system) pathways increased in the T2 group compared to the T0 group. All the mentioned pathways are involved in ATP production. All cells use ATP as an energy source for survival, proliferation, and differentiation. ATP and other metabolites can pass directly from CCs to oocytes through gap junctions<sup>19</sup>—these cumulus-oocyte communications attempt to control COC energy metabolism. Energy production in the COC to sustain meiosis during oocyte maturation and subsequent rapid proliferation of cells during embryonic development before implantation is essential<sup>20</sup>. When these cellular mechanisms are disrupted, molecular damage to the oocyte can induce mitochondrial mutations and reduce ATP production, which is harmful to the oocyte<sup>20</sup>. Albert et al. showed a statistically significant decrease in the ATP level of CCs from individuals with endometriosis undergoing IVF compared to the control group. Also, their study showed a negative correlation between the ATP of CCs and age<sup>21</sup>.

On the other hand, suppression of OXPHOS and reduction of ATP production lead to increased apoptosis and suppression of CC proliferation<sup>22</sup>. By increasing apoptosis in CCs and decreasing the proliferation of these cells, oocytes may not receive proper nutrition from these cells, lead to damage to the oocytes. These data suggest that COCs without pre-incubation may have defects in ATP production and mitochondrial function and increased CCs apoptosis. This may lead to reduced oocyte competence and fertilization rate. It is possible that pre-incubating CCs for 2 h with sufficient ATP production would better support the oocyte. Confirmation of these results requires more extensive studies.

The TNF-alpha signaling pathway was among the pathways that increased in the T2 group compared to the T0 group. The TNF signaling pathway involves several processes, including cell proliferation, apoptosis, differentiation, inflammatory and immune response modulation<sup>23</sup>. The genes were upregulated in this pathway were the TNFAIP3 and BIRC3 genes, both of which are among the apoptosis-inhibiting genes. BIRC3 encodes a member of the inhibitors of apoptosis protein (IAP) family that inhibit apoptosis by binding to tumor necrosis factor receptor-associated factors TRAF1 and TRAF2<sup>24</sup>. Also, the protein encoded by TNFAIP3 is a zinc finger protein and ubiquitin-editing enzyme and has been shown to inhibit NF-kappa B activation as well as TNF-mediated apoptosis<sup>25</sup>. It has been reported that TNFAIP6 and TNFAIP3 are decreased in the CCs of endometriosis patients compared to healthy individuals, which may be related to low embryo quality in these patients<sup>23,26</sup>. Increased apoptosis in CCs can lead to abnormalities in cleavage divisions of the embryo<sup>27,28</sup>. Gametes and embryos obtained from COCs without apoptosis or with a minimal amount of apoptosis increase the probability of reaching the blastocyst stage<sup>29</sup>. With increased apoptosis in CCs, the oocyte may not receive proper nutrition from these cells. Also, increased apoptosis of CCs has been associated with abnormal oocyte morphology<sup>30</sup>, abnormal embryo cleavage<sup>28</sup>, reduction of fertilization<sup>31</sup>, and blastocyst rate<sup>29</sup>. In addition, the expression level of pro-apoptotic genes in cumulus cells of low-quality embryos was higher than in high-quality embryos<sup>32</sup>. Based on this, apoptosis in CCs of the T2 group may be less than that of the T0 group. For this reason, the effectiveness of these cells in supporting oocytes is higher in this group.

In the T2 group and the T0 group of our study, one of the pathways that increased was the glucocorticoid receptor pathway. Glucocorticoids (GCs) involve essential processes such as transcription, energy metabolism, and apoptosis. The GC receptor, NR3C1, can bind to DNA and modulate pathways related to these processes. These compounds regulate oxidative phosphorylation gene expression, which is essential in physiological processes that require energy, such as lipid metabolism, stress response, and reproduction. GCs have a unique role in the early stages of reproduction, and NR3C1 has been found to be highly expressed in primordial and antral follicles. ROS imbalance caused by stressful events can alter GC regulation and negatively affect oocyte competence. GC also has an anti-inflammatory effect on ovarian follicular cells and protects the cells from apoptotic signals. The anti-inflammatory effect of GCs is exerted by two complementary mechanisms: induction of apoptosis of inflammatory cells and arrest of apoptosis in resident cells of inflamed tissue. Although the mechanism of GC action on oocyte maturation remains controversial, it has been evaluated positively in horse and mouse species oocytes. Also, in zebrafish, GC receptor knockout led to impaired ovulation, oocyte maturation and defects in fertility.

Furthermore, the knockdown of NR3C1 inhibits the proliferation of cumulus cells<sup>33</sup>. Proper expansion of CCs is essential for fertility. An expanded cumulus cell is required for ovulation, and it facilitates oocyte extrusion during ovulation, transfer to the fertilization site, and sperm penetration. Cumulus expansion is also related to oocyte competence<sup>34</sup>. Based on this, the CCs of COCs T2 pre-incubation may have more CCs expansion and less apoptosis, inflammation, leading to the production of competent oocytes with better support from oocytes.

Studies have shown that the exposure of COC's cumulus cells to hydrogen peroxide before fertilization reduced the cleavage rate of the embryo. Also, exposure of the oocyte to hydrogen peroxide leads to the death of the oocyte and defects in the first cleavage<sup>35</sup>. Lin et al. showed that ROS increases in granulosa cells of endometriosis patients, which causes cellular senescence and contributes to endometriosis-related infertility<sup>36</sup>. These studies show that CCs protect the oocyte against oxidative stress, and that increased reactive oxygen species in CCs can lead to defects in this support<sup>35,36</sup>. Transforming growth factor (TGF)- $\beta$  is one of the factors that leads to an increase in the production of reactive oxygen species (ROS) and a decrease in the concentration of glutathione (GSH) in different types of cells. NAD(P)H oxidase (NOX) is one of the sources of ROS, and TGF- $\beta$  leads to an increase in ROS through its effect on NOX. This relationship is two-way, and the increase in ROS also leads to a rise in TGF- $\beta$  gene expression<sup>37</sup>. TGF receptor is one of the pathways that decreased in our study in the T2 group compared to the T0 group. The upregulation of this pathway in the T0 group may lead to an increase in ROS in the CCs of this group and decrease their ability to support the oocyte.

Many studies have shown that oocyte pre-incubation is effective on oocyte and embryo quality, but the appropriate pre-incubation time is not precisely known. In this study, the effect of 2 h of pre-incubation was investigated and compared with no incubation. The results showed that 2 h leads to changes in important pathways in CCs, which may positively affect oocyte quality. Therefore, T2 pre-incubation may lead to better

support of the CCs to the oocyte and thus to a more complete maturation of the oocyte, and more research in this field seems necessary. One of the limitations of this study was the impossibility of direct transcriptomics analysis of oocytes due to ethical problems. Another limitation of this study was the small sample size. It is suggested that more incubation times be compared in future studies and that the examination of the genes and pathways be done in a more specific way. It is also suggested that the functional validation of essential genes be included in the project.

### Data availability

The datasets generated and analyzed during the current study are available in the GEO repository, [<https://www.ncbi.nlm.nih.gov/geo/query/acc.cgi?acc=GSE252038>] with GEO accession GSE252038.

Received: 12 February 2024; Accepted: 4 July 2024

Published online: 26 July 2024

### References

- Meng, Q. *et al.* Incidence of infertility and risk factors of impaired fecundity among newly married couples in a Chinese population. *Reprod. Biomed. Online* **30**, 92–100 (2015).
- Devjak, R. *et al.* Cumulus cells gene expression profiling in terms of oocyte maturity in controlled ovarian hyperstimulation using GnRH agonist or GnRH antagonist. (2012).
- Falcone, P. *et al.* Correlation between oocyte preincubation time and pregnancy rate after intracytoplasmic sperm injection. *Gynecol. Endocrinol.* **24**, 295–299 (2008).
- Mohammadi, F. *et al.* The effect of preincubation time and myo-inositol supplementation on the quality of mouse mii oocytes. *J. Reprod. Infertil.* **21**, 259 (2020).
- Ho, J.Y.-P., Chen, M.-J., Yi, Y.-C., Guu, H.-F. & Ho, E.S.-C. The effect of preincubation period of oocytes on nuclear maturity, fertilization rate, embryo quality, and pregnancy outcome in IVF and ICSI. *J. Assist. Reprod. Genet.* **20**, 358–364 (2003).
- Isiklar, A. *et al.* Impact of oocyte pre-incubation time on fertilization, embryo quality and pregnancy rate after intracytoplasmic sperm injection. *Reprod. Biomed. Online* **8**, 682–686 (2004).
- Watanabe, H. Correlation between the number of cultured human embryos and embryo development in the wow culture dish system. *Fertil. Steril.* **108**, e158 (2017).
- Govahi, A. *et al.* Cutting-edge techniques provide insights regarding repeated implantation failure patients. *Reprod. Biomed. Online* **46**, 687–696 (2023).
- Memili, E. *et al.* Bovine germinal vesicle oocyte and cumulus cell proteomics. *Reproduction* **133**, 1107–1120 (2007).
- Revelli, A. *et al.* Follicular fluid content and oocyte quality: From single biochemical markers to metabolomics. *Reprod. Biol. Endocrinol.* **7**, 1–13 (2009).
- Andrews, S. *et al.* FastQC. *A quality control tool for high throughput sequence data* **370** (2010).
- Kim, D., Langmead, B. & Salzberg, S. L. HISAT: A fast spliced aligner with low memory requirements. *Nat. Methods* **12**, 357–360 (2015).
- Pertea, M., Kim, D., Pertea, G. M., Leek, J. T. & Salzberg, S. L. Transcript-level expression analysis of RNA-seq experiments with HISAT StringTie, and Ballgown. *Nat. Protoc.* **11**, 1650–1667 (2016).
- Ghosh, S. & Chan, C.-K.K. *Analysis of RNA-Seq data using TopHat and Cufflinks* 339–361 (Plant Bioinformatics Methods and Protocols, Springer, New York, 2016).
- Therneau, T., Hart, S. & Kocher, J. P. Calculating sampleSize estimates for RNA Seq studies. R package version 1.10. 0. (2020).
- Chen, E. Y. *et al.* Enrichr: interactive and collaborative HTML5 gene list enrichment analysis tool. *BMC Bioinform.* **14**, 1–14 (2013).
- Thorvaldsdóttir, H., Robinson, J. T. & Mesirov, J. P. Integrative genomics viewer (IGV): High-performance genomics data visualization and exploration. *Brief. Bioinform.* **14**, 178–192 (2013).
- Adolfsson, E. & Andershed, A. N. Morphology vs morphokinetics: A retrospective comparison of inter-observer and intra-observer agreement between embryologists on blastocysts with known implantation outcome. *JBRA Assist. Reprod.* **22**, 228 (2018).
- Dunning, K. R., Russell, D. L. & Robker, R. L. Lipids and oocyte developmental competence: the role of fatty acids and  $\beta$ -oxidation. *Reproduction* **148**, R15–27 (2014).
- Imanaka, S., Shigetomi, H. & Kobayashi, H. Reprogramming of glucose metabolism of cumulus cells and oocytes and its therapeutic significance. *Reprod. Sci.* **29**, 653–667 (2022).
- Hsu, A. L., Townsend, P. M., Oehninger, S. & Castora, F. J. Endometriosis may be associated with mitochondrial dysfunction in cumulus cells from subjects undergoing in vitro fertilization-intracytoplasmic sperm injection, as reflected by decreased adenosine triphosphate production. *Fertil. Steril.* **103**, 347–352 (2015).
- Zhou, X. *et al.* MiR-126-3p inhibits apoptosis and promotes proliferation by targeting phosphatidylinositol 3-kinase regulatory subunit 2 in porcine ovarian granulosa cells. *Asian-Australas. J. Animal Sci.* **33**, 879 (2020).
- Da Luz, C. M. *et al.* Transcriptomic analysis of cumulus cells shows altered pathways in patients with minimal and mild endometriosis. *Sci. Rep.* **12**, 5775 (2022).
- Diop, F. *et al.* Biological and clinical implications of BIRC3 mutations in chronic lymphocytic leukemia. *Haematologica* **105**, 448 (2020).
- Verstrepen, L. *et al.* Expression, biological activities and mechanisms of action of A20 (TNFAIP3). *Biochem. Pharmacol.* **80**, 2009–2020 (2010).
- Allegra, A. *et al.* The gene expression profile of cumulus cells reveals altered pathways in patients with endometriosis. *J. Assist. Reprod. Genet.* **31**, 1277–1285 (2014).
- Burrows, A. E. *et al.* The *C. elegans* Myt1 ortholog is required for the proper timing of oocyte maturation. (2006).
- Faramarzi, A., Khalili, M. A. & Jahromi, M. G. Is there any correlation between apoptotic genes expression in cumulus cells with embryo morphokinetics?. *Mol. Biol. Rep.* **46**, 3663–3670 (2019).
- Corn, C. M., Hauser-Kronberger, C., Moser, M., Tews, G. & Ebner, T. Predictive value of cumulus cell apoptosis with regard to blastocyst development of corresponding gametes. *Fertil. Steril.* **84**, 627–633 (2005).
- Luo, Y. *et al.* CTC1 increases the radioresistance of human melanoma cells by inhibiting telomere shortening and apoptosis. *Int. J. Mol. Med.* **33**, 1484–1490 (2014).
- Høst, E., Gabrielsen, A., Lindenberg, S. & Smidt-Jensen, S. Apoptosis in human cumulus cells in relation to zona pellucida thickness variation, maturation stage, and cleavage of the corresponding oocyte after intracytoplasmic sperm injection. *Fertil. Steril.* **77**, 511–515 (2002).
- Govahi, A., Amjadi, F., Nasr-Esfahani, M.-H., Raoufi, E. & Mehdizadeh, M. Accompaniment of time-lapse parameters and cumulus cell RNA-sequencing in embryo evaluation. *Reprod. Sci.* **29**, 1–15 (2022).



33. Ruiz-Conca, M., Gardela, J., Mogas, T., López-Béjar, M. & Álvarez-Rodríguez, M. Apoptosis and glucocorticoid-related genes mRNA expression is modulated by coenzyme Q10 supplementation during in vitro maturation and vitrification of bovine oocytes and cumulus cells. *Theriogenology* **192**, 62–72 (2022).
34. Richani, D., Dunning, K. R., Thompson, J. G. & Gilchrist, R. B. Metabolic co-dependence of the oocyte and cumulus cells: Essential role in determining oocyte developmental competence. *Human Reprod. Update* **27**, 27–47 (2021).
35. Fatehi, A. N. *et al.* Presence of cumulus cells during in vitro fertilization protects the bovine oocyte against oxidative stress and improves first cleavage but does not affect further development. *Zygote* **13**, 177–185 (2005).
36. Lin, X. *et al.* Excessive oxidative stress in cumulus granulosa cells induced cell senescence contributes to endometriosis-associated infertility. *Redox Biol.* **30**, 101431 (2020).
37. Liu, R.-M. & Pravia, K. G. Oxidative stress and glutathione in TGF- $\beta$ -mediated fibrogenesis. *Free Radical Biol. Med.* **48**, 1–15 (2010).

## Acknowledgements

The authors would like to thank Iran University of Medical Sciences (IUMS), Tehran, Iran, for their cooperation throughout study.

## Author contributions

M.M.: project administration, designed the study, and reviewed the manuscript. A.G.: performed the experiments and wrote the paper. S.E.: performed the experiments. N.E.G.H. and Z.Z.: The study was designed, and the data was analyzed. M.A.: reviewed the manuscript. R.M.: data collection.

## Funding

This work was supported by the Iran University of Medical Sciences (grant no. 31837).

## Competing interests

The authors declare no competing interests.

## Additional information

**Correspondence** and requests for materials should be addressed to M.M.

**Reprints and permissions information** is available at [www.nature.com/reprints](http://www.nature.com/reprints).

**Publisher's note** Springer Nature remains neutral with regard to jurisdictional claims in published maps and institutional affiliations.



**Open Access** This article is licensed under a Creative Commons Attribution-NonCommercial-NoDerivatives 4.0 International License, which permits any non-commercial use, sharing, distribution and reproduction in any medium or format, as long as you give appropriate credit to the original author(s) and the source, provide a link to the Creative Commons licence, and indicate if you modified the licensed material. You do not have permission under this licence to share adapted material derived from this article or parts of it. The images or other third party material in this article are included in the article's Creative Commons licence, unless indicated otherwise in a credit line to the material. If material is not included in the article's Creative Commons licence and your intended use is not permitted by statutory regulation or exceeds the permitted use, you will need to obtain permission directly from the copyright holder. To view a copy of this licence, visit <http://creativecommons.org/licenses/by-nc-nd/4.0/>.

© The Author(s) 2024